

Urban Safety Perception Through the Lens of Large Multimodal Models: A Persona-based Approach

Ciro Beneduce,^{1,2} Bruno Lepri,¹ and Massimiliano Luca^{1,*}

¹*Fondazione Bruno Kessler, Via Sommarive 18, 38123 Povo (TN), Italy*

²*University of Trento, Department of Information Engineering and Computer Science, Via Sommarive 9, 38123 Povo (TN), Italy*

Understanding how urban environments are perceived in terms of safety is crucial for urban planning and policymaking. Traditional methods like surveys are limited by high cost, required time, and scalability issues. To overcome these challenges, this study introduces Large Multimodal Models (LMMs), specifically Llava 1.6 7B, as a novel approach to assess safety perceptions of urban spaces using street-view images. In addition, the research investigated how this task is affected by different socio-demographic perspectives, simulated by the model through Persona-based prompts. Without additional fine-tuning, the model achieved an average F1-score of 59.21% in classifying urban scenarios as safe or unsafe, identifying three key drivers of perceived unsafety: isolation, physical decay, and urban infrastructural challenges. Moreover, incorporating Persona-based prompts revealed significant variations in safety perceptions across the socio-demographic groups of age, gender, and nationality. Elder and female Personas consistently perceive higher levels of unsafety than younger or male Personas. Similarly, nationality-specific differences were evident in the proportion of unsafe classifications ranging from 19.71% in Singapore to 40.15% in Botswana. Notably, the model’s default configuration aligned most closely with a middle-aged, male Persona. These findings highlight the potential of LMMs as a scalable and cost-effective alternative to traditional methods for urban safety perceptions. While the sensitivity of these models to socio-demographic factors underscores the need for thoughtful deployment, their ability to provide nuanced perspectives makes them a promising tool for AI-driven urban planning.

INTRODUCTION

Understanding how people perceive urban spaces is a crucial area of research, particularly for urban planners aiming to develop citizen-centric cities [1–3]. Traditionally, surveys have been the primary tool for assessing urban perceptions [4–6]. However, these approaches often focus on planned developments or specific conditions (e.g., time of day) and are constrained by high costs, time-consuming data collection, and limited scalability. Moreover, cities evolve rapidly, and even minor changes—such as the opening or closing of a business—can influence how crowds and individuals navigate

* Corresponding author: mluca@fbk.eu

and experience urban environments [7–9]. Given the dynamic nature of urban spaces, surveys alone may not be the most effective tool for capturing real-time perceptions.

To address these limitations, researchers have increasingly explored alternative data sources. One promising approach involves integrating Street-View Images (SVIs) with computer vision techniques to tackle various urban challenges, such as socioeconomic estimation [10], pedestrian environment assessment [11], and flood risk evaluation [12]. SVIs have also been leveraged to analyze urban perception, providing insights into how individuals perceive safety, aesthetics, and livability across different cityscapes [13–17]. Previous studies have employed machine learning and deep learning models to estimate safety perception scores from images [13, 18, 19]. However, perception is inherently influenced by socio-demographic factors [20], which have been shown to shape attitudes toward environmentalism [21–24], tourism [25, 26], health [27, 28], and broader urban experiences [29–31]. While the data collection processes in some studies include socio-demographic information [14], the predictive models themselves rely solely on image content, without incorporating these additional variables, and the social dimension is only used as a control variable or to understand human behaviors with respect to perception [32]. The emergence of Large Multimodal Models (LMMs) such as Llava 1.6 [33, 34], presents a new opportunity to bridge this gap. Indeed, other researchers showed that language encoders can be used to design Personas in prompts to diversify the outputs [35–37] and to successfully mimic human behavior [38–40].

In our study, we first determine if Llava 1.6 7B can estimate urban safety perception by measuring models’ performances in terms of F1-score using SVIs from the Place Pulse 2.0 dataset [15]. Despite various Large Multimodal Models, in our work, we selected Llava 1.6 [41, 42] in its 7 billion parameters version. Llava is one of the prominent LMM models and achieves state-of-the-art performances on 11 benchmarks [42]. In addition, the smallest version of Llava 1.6 consists of 7 billion parameters. Thus, it is possible to reproduce our task on small GPUs at contained costs. We chose Place Pulse 2.0 over other datasets (e.g., [18]) because its safety perception scores are derived directly from survey-like data collection, providing a closer alignment with human perception. Without specifying any socio-demographic characteristic of the potential *observer*, Llava 1.6 achieves F1-scores up to 72.31% in single cities. Building on this, we introduce Persona-based prompts to examine how socio-demographic characteristics influence safety perception.

Our results show clear patterns in perception differences across nationality, gender, and age prompts. There is a noticeable discrepancy in the way different country-based Personas classify the same images, with a clear pattern toward a greater perception of insecurity for developing and poorer nations. Concerning gender, we find that specifying the Persona identity as a female tends to have higher unsafe predictions compared to the male Persona. Similarly, by prompting age bins, we observe that older Personas perceive the selected SVIs more unsafely with respect to middle-aged and young Personas. Also, we do not observe significant differences between middle-aged and young Personas. Interestingly, we also find that if we do not specify a Persona, the answers to the Neutral prompt are

particularly aligned with middle-aged/young males. Finally, we analyze the keywords provided by the model to better understand which aspect of the SVIs is considered when making a decision. Surprisingly, our findings show an alignment with well-known theories from social science like Jacobs’ “Eyes on the Streets” [43] and Wilson and Kelling’s “Broken Windows” [44].

As foundation models are increasingly deployed in urban planning and other numerous real-world applications, this result is of paramount relevance and further highlights the importance of carefully designing prompts and specifying Personas to ensure the relevant population is considered when making urban planning decisions.

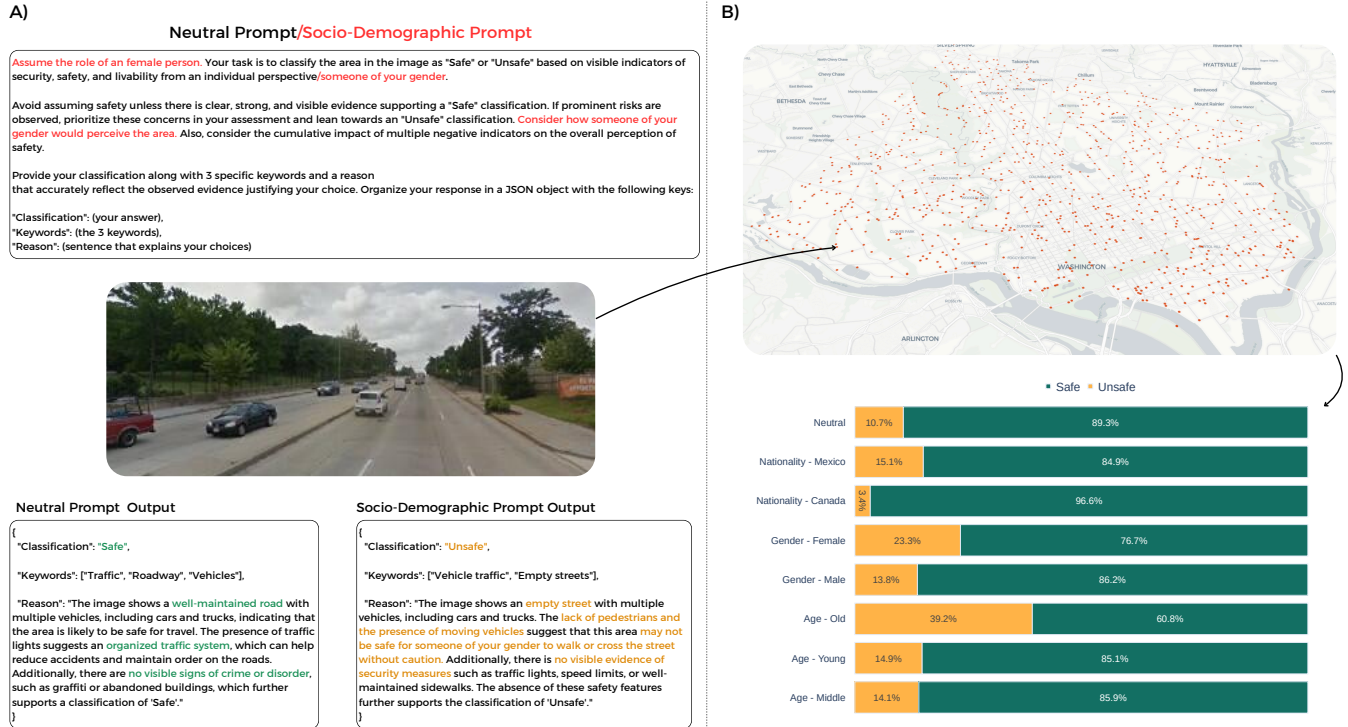


Figure 1. **Panel A** compares the neutral prompt (black text) with the socio-demographic prompt (red highlights), specifically focusing on a female Persona. The comparison showcases differences in classification, keywords, and reasoning for the same image. **Panel B** aggregates these differences to a city-level analysis in Washington, D.C., visualizing how classifications shift across demographics. The bar chart highlights variations in safety perception across genders, age groups, and nationalities, emphasizing the disparities in outcomes for *Safe* versus *Unsafe* classifications.

RESULTS

A. Predicting Safeness Perception with Large Multimodal Models

Our study primarily investigates the capabilities of Llava 1.6 [33] in classifying perceived safety in urban environments, utilizing Place Pulse 2.0 as the source of SVIs and ground truth data. A detailed description of the model, dataset, and true ground thresholding is provided in the Materials and Methods section.

After, we design a prompt capable of performing a binary classification and establishing if a place is *safe* or *unsafe*.

Such prompt is henceforth referred to as *Neutral prompt* and aims at classifying the SVI without considering any socio-demographic information. The prompt is described in Materials and Methods and can be seen in Figure 1. By inputting an SVI and the Neutral prompt to the LMM, we achieve an overall F1-score of 59.21%, a precision of 55.48%, and a recall of 66.83%. Given the class imbalance in Place Pulse 2.0, we selected the F1-score as our primary performance metric. Although accuracy is widely used, it can be misleading in imbalanced datasets, as it tends to overestimate performance by favoring the majority class [45]. By using the F1-score, we account for both false positives and false negatives, ensuring a more reliable assessment. All reported results represent the average performance across two experimental runs. The obtained performances highlight that we can use Llava 1.6 to classify safety perception. To reach such performances, unlike conventional approaches that rely on computer vision models explicitly trained to extract safety-related features [13–15, 17], we did not fine-tune or retrain the LMM.

Interestingly, we notice a significant variability in the model’s performance across cities. Indeed, the overall F1-score is 59.21%, but city-wise, as detailed in Supplementary Note S1 and Supplementary Table S1. The highest F1-score is observed in Minneapolis (72.31%), followed by Denver (71.18%) and Toronto (70.29%), while the lowest F1-scores are found in Rio de Janeiro (27.36%), Taipei (30.38%), and Bangkok (31.18%). In Supplementary Table S1, we also report recall and precision scores for each city.

The variability we observe at the city scale suggests that the model may consider specific factors such as urban design, context, and environmental features to make safety perception predictions. This aspect is further confirmed if we analyze the explanations provided by the model, visible in Supplementary Note S3, Supplementary Table S2-S3. Such features, also lead to significant variability in the unsafe classified images for each city, with Denver considered the safest with only 9.54% unsafe images and Rio De Janeiro the unsafest with the 81.70%.

We also explore *where* the places that are perceived unsafe by the model are geographically located. In particular, by considering only the unsafe predictions, we run a hierarchical cluster to spot if certain geographical regions are systematically predicted as unsafer than others. Additional information on the hierarchical clustering technique can be found in Materials and Methods, while the visualization is shown in Supplementary Note S2, Supplementary Figure S1. We found that cities in regions with perceived higher levels of safety, such as parts of North America, Western and Northern Europe, and Australia, often clustered together with a low rate of unsafe classifications. In contrast, cities in South America and Southeast Asia, such as Rio de Janeiro and Bangkok, form a distinct cluster characterized by the highest unsafe classifications. Interestingly, Southern Europe (Rome, Lisbon), East Asia (Tokyo, Kyoto), and Latin America (Santiago) fall into an intermediate cluster, reflecting moderate-high unsafe scores. Finally, a separate cluster emerged for a mixture of cities, such as Mexico City, Moscow, and Bucharest. This group exhibited higher unsafe classification scores than the intermediate cluster but did not reach the extremes observed in South America and Southeast Asia.

B. Drivers of Unsafety

sense of safety and accessibility in these areas. The second community emphasizes orderliness and aesthetic upkeep, with central terms such as "well-maintained," "orderly," and "secure". Keywords like "low crime" and "residential area" further reinforce the perception of these areas as visually appealing and inherently safe. In contrast, Community 3 is dominated by general themes of urban development and infrastructure, with all the nodes perfectly connected.

On the other hand, the unsafe network exhibits a different thematic structure, highlighting concerns associated with neglect, isolation, and urban decay. The first community within the unsafe network focuses on vandalism and social isolation, as reflected by central nodes such as "isolated", "abandoned", and "neglected." The second community underscores visible signs of disorder and poor upkeep, with keywords like "empty", "lack of maintenance", and "security concerns" dominating the network. Lastly, also in this case the third community deals with urban infrastructure challenges, with all the nodes having the same degree of centrality.

Interestingly, Community 3 in both networks is very similar, suggesting that urban infrastructure is a shared theme across both classifications. However, its interpretation varies depending on the context and the other nodes connected. In the safe network, infrastructure is associated with organized and well-maintained urban spaces, whereas, in the unsafe network, it is linked to physical decay, isolation, and vandalism.

1. *Alignment with Urban Criminology and Social Theories*

The findings of the network analysis align the linguistic cues in the model's outputs with historical theories from urban criminology and sociology, including Kelling and Wilson's Broken Windows theory [44], Jacobs' Eyes on the Street [43], Newman's Defensible Space theory [46] and Social Disorganization Theory [47, 48].

Broken Windows theory underscores the importance of visible order, which aligns with the safe network's emphasis on well-maintained and orderly environments as indicators of security and livability. Conversely, the unsafe network reflects the theory's assertion that visible signs of disorder can lead to perceptions of insecurity and further neglect. Similarly, Jane Jacobs' Eyes on the Street theory highlights the role of active and engaged urban spaces in promoting safety. The safe network nodes, such as 'neighborhood' and 'residential', support this view, emphasizing the importance of active, well-populated environments in creating natural surveillance and deterring crime. The unsafe network's themes of 'vacant', 'isolated', and 'lack of pedestrians' illustrate the challenges posed by desolate spaces, strengthening Jacobs' assertion of the dangers of the elimination of pedestrian activity. Additionally, Newman's Defensible Space Theory underlines the significance of architectural and spatial design in creating secure environments, perfectly illustrating the contrasting roles of Community 3 shared by the two networks. While in the safe network, these elements could allow organization and accessibility, their design or maintenance in the unsafe network suggests disorder and inefficiencies that undermine the perception of safety.

Finally, Social Disorganization Theory adds another layer of insight by positing that crime is more likely to rise in communities where social cohesion is weakened by factors such as economic disadvantage, residential instability,

and high unemployment. In our analysis, the safe network’s emphasis on community engagement and neighbourhood suggests a robust social fabric that deters criminal behaviour. On the other hand, the unsafe network’s focus on isolation and vandalism, explicitly citing "gated community", mirrors the breakdown in social cohesion that Social Disorganization Theory associates with higher crime rates.

C. The Role of Personas

Zero-shot learning, a paradigm where models make predictions on tasks without prior task-specific training, has been increasingly explored in various domains [49–51]. Previously, we demonstrated that LMMs can assess urban safety perception in a zero-shot fashion, meaning we evaluate safety by directly prompting the model and without any fine-tuning related to the dataset (i.e., SVIs) or task (i.e., safety perception). However, a critical question emerges: *whose* perception is being captured? Contemporary urban planning increasingly embraces citizen-centric approaches and co-design methodologies [2, 3, 52, 53], while foundation models are becoming prevalent across various domains as decision-support tools and process managers [54, 55]. Therefore, understanding whether we can model different Personas within prompts and quantifying the impact of socio-demographic factors on the results becomes crucial.

In this study, we investigate the variability in safety perception across different socio-demographic characteristics (nationality, gender, and age cohorts). Our findings reveal that all these characteristics significantly influence safety perception, with some factors showing particularly pronounced effects. Most notably, we discover that responses obtained using the *Neutral prompt* align predominantly with those from young and middle-aged male respondents. This alignment, potentially, indicates an inherent model bias.

The detailed results for each socio-demographic prompt are presented in the following sections.



Figure 3. Multi-panel visualization analyzing unsafe image classifications, keyword frequency by gender, and contextual reasoning based on age-based Personas. (A) Unsafe Percentage by Nation: A horizontal bar plot showing the percentage of images classified as unsafe across nationality prompts, with error bars representing variability across runs. (B) Keyword Frequency Comparison: A grouped bar chart illustrating gender-based differences in keyword associations, such as higher frequencies of *Isolated* and *Deserted* for female prompts, and *Residential* and *Well-maintained* for male prompts. (C) Age-Prompt-Based Classification of the Same Image: this panel demonstrates how the same image (top) is classified differently based on three distinct age-based prompts. The classifications range from *Safe* for younger and middle-aged prompts to *Unsafe* for elder prompts, demonstrating the model’s sensitivity to the Persona age. The keywords and reasoning highlight the model’s reliance on environmental factors such as pedestrian activity, urban maintenance, and surveillance presence. For instance, younger Personas emphasize accessibility and human activity, while elder Personas are influenced by isolation and the lack of visible security measures, resulting in differing perceptions of safety.

1. Nationality

We modify the prompt as described in Materials and Methods section and as shown in the example of Supplementary Note S4, Supplementary Table S4 to capture socio-demographic factors like a person’s nationality, age bin, or gender. In this first experiment, we specify in the prompt to evaluate the image as if the person is raised and born in a specific nation. We test 32 nationalities corresponding to the nations of the 56 analyzed cities. The full list of nationalities we tested can be found in Supplementary Note S6, Supplementary Table S11. For each specified nationality, the model systematically evaluates all images in the dataset through the lens of that cultural perspective. For instance, when the prompt defines a Persona born and raised in Brazil, the model reassesses every image across all cities from a Brazilian

viewpoint.

The findings reveal substantial differences in perceptions of safety among nationalities, as shown by the proportion of images identified as unsafe by the model, averaged across all cities, in Figure 3. Notably, the proportion of *Unsafe* classified images varies significantly across countries. In Singapore, which receives the safest classifications, only 19.71% of images are labelled as *Unsafe*. In contrast, Botswana, the unsafest classified country, has more than twice this proportion, with 40.15% of images deemed *Unsafe*.

Interestingly, nationalities associated with highly regulated and orderly environments, such as Singapore (19.71%), Canada (21.10%), and Finland (23.28%), tend to classify fewer urban spaces as unsafe. On the other hand, the top three nationalities with the highest percentage of unsafe classifications are Botswana, South Africa, and Mexico, with 40.14%, 39.27%, and 37.05%, respectively. At first glance, this disparity may seem counterintuitive, as one might expect individuals from countries with higher crime rates or less urban infrastructure to be more used to environments perceived as unsafe. However, upon analyzing the reasons provided by the model, it becomes evident that these classifications are influenced by what the model interprets as local or regional characteristics. For instance, Personas from countries with higher crime rates or socio-economic disparities reflect a higher sensitivity towards subtle environmental cues, such as poor lighting, visible neglect, or low pedestrian activity, associating them with potential risks. As a result, they tend to classify a higher proportion of urban spaces as *Unsafe*. Some examples of the model’s reasons are reported in Supplementary Note S5, Supplementary Table S7.

In addition, clustering nationalities based on their average unsafe classification percentages and standard deviations across cities revealed distinct patterns in how different groups perceive urban safety. Figure 4 illustrates seven clusters encompassing the 32 nationalities, reflecting macro-regional and cultural similarities. Nationalities from Northern and Western Europe, for instance, formed clusters characterized by low average unsafe classifications and minimal variability, aligning with perceptions shaped by order and cleanliness. In contrast, nationalities from developing countries clustered together with higher unsafe classifications. These clusters show that the model’s interpretation of urban safety is shaped by shared characteristics within each group, including geographic, environmental, and cultural factors.

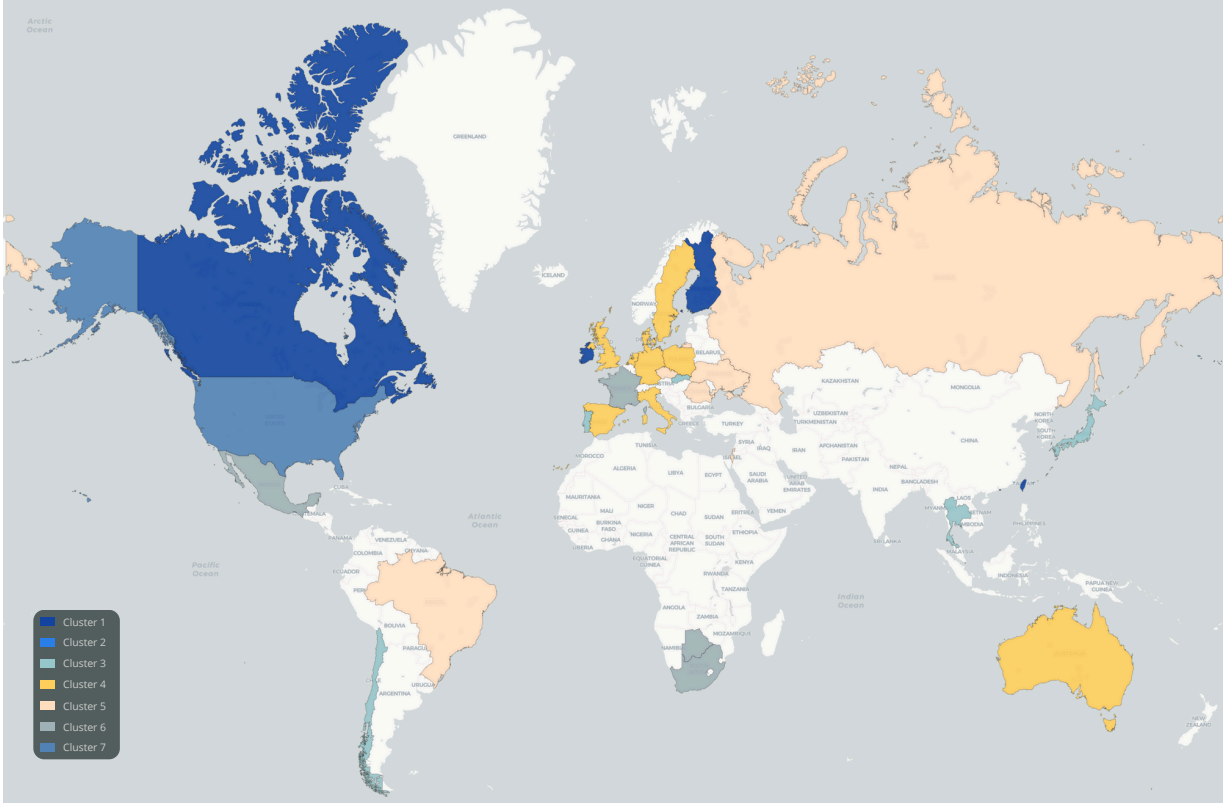


Figure 4. Clustering of 32 nationalities into seven distinct groups based on their unsafe classification percentages and standard deviations across cities, reflecting macro-regional and cultural similarities in urban safety perceptions according to Llava 1.6 7B. Cluster 1 (Taiwan, Canada, Finland, Hong Kong, Ireland) shows consistently low unsafe classifications and minimal variability, while Cluster 6 (Mexico, France, South Africa and Botswana) reveals higher unsafe classifications and greater variability. Cluster 4 (European countries and Australia) demonstrates moderate unsafe classifications along with Cluster 5 (Israel, Romania, Russia, Czech Republic, Brazil, Ukraine), which is perceived as slightly unsafer. Notably, both Singapore and United States formed their own clusters, respectively Cluster 2 and 7.

Digging deeper, we found a positive Pearson’s correlation (0.745) between the average unsafe percentage and its standard deviation across cities. In other words, prompts associated with higher average unsafe classifications tended also to exhibit greater variability across all cities. Potentially, when the model considers that a nationality aligns with unsafe conditions, small differences in images become more impactful, causing swings in its unsafe classifications.

2. Gender

Gender is another factor that may influence safety perception. While identifying individuals with only two genders is not exhaustive, we limited the tested prompts to male and female Personas. We found significant differences in terms of safety perception by specifying the gender. Female prompts yielded a higher proportion of unsafe classifications (48.78%), averaged across all cities, compared to male prompts (36.86%), suggesting that female Personas tend to interpret urban spaces as riskier.

To better understand the factors driving the divergence in safety perception based on gender, we focused on instances

where the model’s classifications differed between male and female prompts. By isolating these cases of disagreement, we analyzed the associated keywords to identify the features that influenced each perspective. The results, illustrated in Figure 3, reveal distinct patterns in how the model interprets urban safety for different genders.

For male prompts, keywords such as "Residential", "Well-maintained" and "Orderly" dominated, emphasizing features of accessibility and organization. These keywords align with a focus on structural and environmental stability, often associated with positive perceptions of safety. In contrast, female prompts showed a stronger emphasis on terms like "Isolated", "Empty streets" and "Lack of Pedestrians" which reflect a sense of vulnerability in urban environments.

3. Age bin

The model’s perspective changes considerably when prompted to adopt an age-specific Persona. Also in this case, we examined the average unsafe classification across cities and their standard deviations for the Young Age, Middle Age, and Elder Age Personas. The Elder Age Persona recorded the highest average unsafe classification percentage at 65.79%, suggesting that the model perceives urban environments as significantly riskier from the perspective of older individuals. In contrast, the Middle Age and Young Age Personas yielded much lower and nearly identical unsafe classification averages of 38.53% and 38.35%, respectively. An example of how the classifications and the perception of the models are influenced by the Age-Persona is provided in Figure 3, panel C, which highlights how the reasons change across Age-Personas for the same image.

D. Neutral Prompt is a Middle Age Male

To discern the impact of socio-demographic Personas, we compared their performance against the *Neutral prompt* of the model. This analysis was designed to uncover how socio-demographic prompts influence unsafe classifications and the overall consistency of the model. Additionally, it aimed to identify which Personas demonstrate the closest alignment with the model’s standard configuration.

Initially, we evaluated the internal consistency of city rankings based on their unsafe classification percentages across all prompts. Using Spearman rank correlation, we observed high consistency (0.976), indicating that despite variations in unsafe percentages across prompts, the relative city rankings remained stable.

Furthermore, we employed the *Delta Unsafe* metric to assess the deviation of various prompts from a neutral baseline in terms of their unsafe classification rates (refer to Materials and Methods for additional details). To enhance clarity, we aggregated data at the country level for nationalities, setting the neutral baseline as the zero reference point (Figure 5, Panel A).

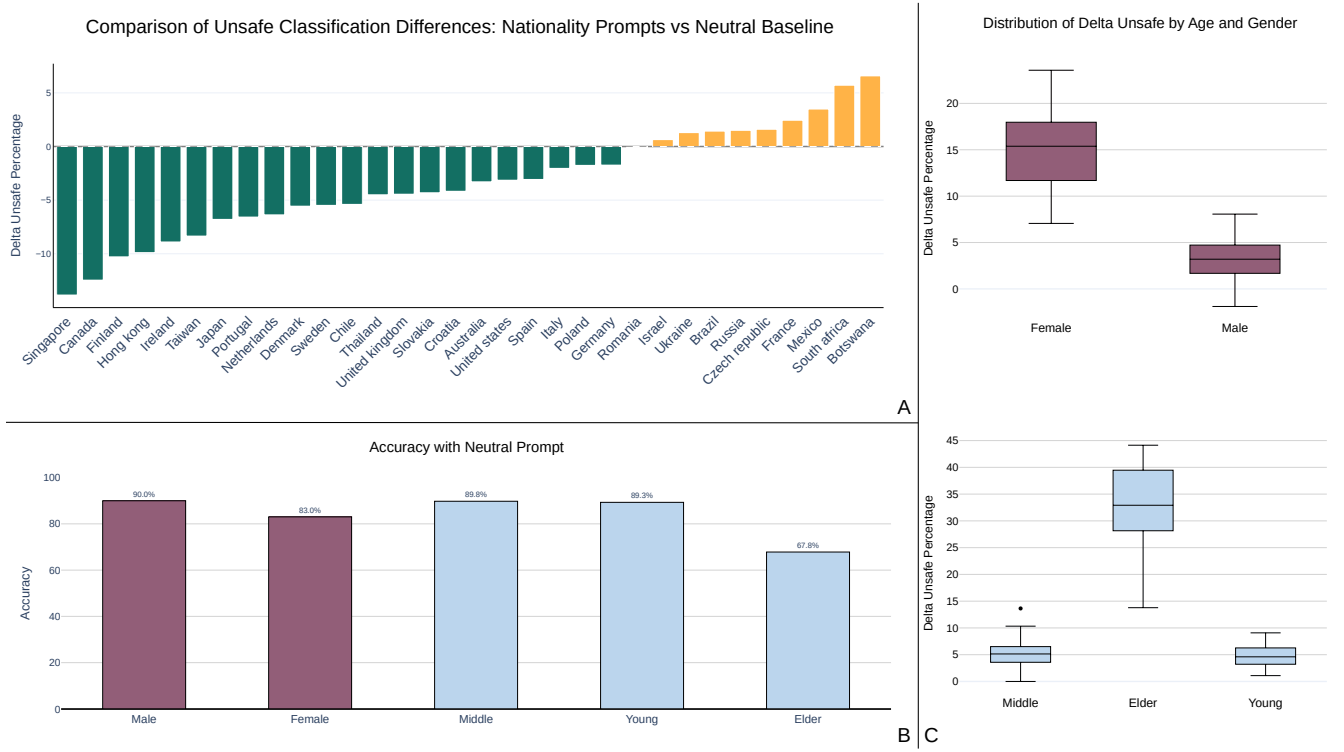


Figure 5. Multi-panel visualization analyzing the impact of different demographic prompts (nationality, gender, and age) on unsafe classifications and accuracy compared to a neutral baseline. (A) Nationality-Based Unsafe Classification Differences: A bar chart comparing the difference in unsafe classification rates between various nationality prompts and a neutral baseline. Negative values (green bars) indicate lower unsafe classification rates than neutral, while positive values (orange bars) indicate higher unsafe classification rates, suggesting that certain nationality prompts lead to greater perceived unsafety. (B) Accuracy with Neutral Prompt: A grouped bar chart displaying the classification accuracy for gender and age prompts when compared to a neutral reference. Male and Middle-Aged prompts exhibit the highest accuracy, while Elder prompts show the lowest accuracy, suggesting potential disparities in model robustness across demographic attributes. (C) Age- and Gender-Based Unsafe Classification Distributions: Boxplots showing the distribution of unsafe classification differences for gender (top) and age (bottom) prompts. Female prompts tend to have a higher median unsafe classification difference than male prompts. Similarly, the Elder age group exhibits the widest range and highest median unsafe classification differences.

This approach highlights distinct differences: for instance, Singapore and Canada exhibit notably lower unsafe classification rates with decreases of 13.85% and 12.46%, respectively, suggesting safer perceptions compared to the baseline. Conversely, Botswana and South Africa show increases in unsafe rates of 6.59% and 5.71%, respectively, indicating higher perceived risks. Countries like Romania, Israel, and Ukraine align closely with the neutral baseline, showing changes of -0.09% , $+0.64\%$, and $+1.30\%$, respectively, which suggests minimal perceptual shifts from the neutral assessment.

In a similar manner, our analysis further explores how perceptions of safety differ according to demographic factors (Figure 5, Panel B). This evaluation is conducted at both the city level, considering individual cities separately, and across aggregated data that combines results from all cities within each demographic category. The results reveal significant variances: the *Female* prompt, for instance, showed a substantial increase in the *Delta Unsafe* metric by 15.21%, indicating a higher perceived risk compared to the *Male* prompt, which only increased by 3.29%. Among the Age-based prompts, the *Elder* Persona is perceived as markedly less safe, with a 32.22% deviation from the neutral

baseline, while the *Middle* and *Young* categories exhibit smaller deviations, indicating perceptions closer to the neutral viewpoint.

Lastly, we conducted an instance-level analysis to evaluate the accuracy of socio-demographic prompts in comparison to the neutral configuration, which was used as the ground truth. The results highlighted discrepancies again. *Male* prompts reached an average accuracy of 90.0%, whereas *Female* prompts were less accurate at 83.0%. Similarly, *Middle* and *Young* age groups showed high accuracies of 89.8% and 89.3%, respectively, while the *Elder* category dropped to 67.8% in accuracy.

These results align closely with earlier observations of *Delta Unsafe* percentages and perfectly underline how the *Neutral prompt* functions as a reference case for *Male* and *Middle-aged* Personas, consistently showing higher alignment. Therefore, these findings highlight the critical importance of explicitly specifying socio-demographic characteristics in studies with societal implications. Relying solely on the standard configuration of the model risks failing to capture the diversity of demographic groups.

DISCUSSION

Our study explored the potential of LMMs, specifically Llava 1.6 7B, to evaluate urban safety perceptions using SVIs. Llava 1.6 demonstrated the ability to classify urban spaces as *Safe* or *Unsafe*, achieving an F1-score of 59.21%. This showcases the versatility of pre-trained vision-language models to generalize across various urban contexts without additional fine-tuning. A key observation from our results is that Llava 1.6 performs significantly better in developed countries compared to developing regions. Cities in North America, Europe, Canada, Australia, and parts of Asia exhibit higher F1-scores, while cities in Latin America, Africa, and Southeast Asia tend to have lower classification accuracy. One explanation for this trend could be that urban environments in developed countries tend to have clearer visual distinctions between safe and unsafe areas. On the other hand, the reasons for this discrepancy could stem from distortions in data distribution, as foundation models are typically trained on datasets dominated by images from Western countries [56].

Interestingly, the inclusion of socio-demographic Personas in the prompt revealed significant variations in how the same urban environment is perceived, offering insights into influences embedded within the model. Prompts based on nationality demonstrated stark differences, ranging from the Singaporean prompts yielding the lowest unsafe classifications (19.71%) and the Botswanian prompts the highest (40.15%), reflecting the model’s sensitivity to regional stereotypes. Gender-based prompts further showed that *Female* Personas resulted in higher unsafe classifications (48.78%) compared to *Male* Personas (36.86%), while age-based prompts revealed a sharp contrast, with *Older* Personas perceiving urban environments as significantly riskier (65.79%) than *Younger* Personas (~38.5%). Despite these variations, the neutral prompt, designed to reflect the model’s standard configuration without specifying socio-demographic characteristics, aligns most closely with the *middle-aged, male* Persona.

The discrepancies in classification performance across nations and socio-demographic groups align with theories from social psychology, criminology, and cognitive science, reinforcing the idea that LMMs do not operate in a vacuum but instead mirror societal biases [57]. The Stereotype Content Model (SCM) [57], suggests that stereotypes function along two axes: warmth (trustworthiness, sociability) and competence (capability, effectiveness). These dimensions shape how individuals perceive and categorize social groups, leading to specific emotional prejudices and discriminatory behaviors. Our findings closely align with the frameworks proposed by the SCM. Nationality-based biases in safety classification mirror the SCM’s findings that different cultural groups are stereotyped based on their perceived economic and social status, leading to higher unsafe classification rates for the developing world. Similarly, gender-based differences in safety classification align with SCM’s assertion that women are often stereotyped as high in warmth but lower in competence, potentially reinforcing narratives of vulnerability. Age-related biases also correspond to SCM’s theory that older individuals are often perceived as warmer but less competent, which could lead to heightened perceptions of insecurity.

In addition, by analysing the drivers of unsafety, we identified three thematic clusters of risks for the model: (1) physical deterioration and isolation; (2) visible urban neglect; and (3) urban infrastructural challenges. These clusters align closely with criminological theories, such as Kelling and Wilson’s Broken Windows Theory [44]. Furthermore, environments classified as *Safe* featured keywords like "orderly," "residential," and "well-maintained," supporting Jacobs’ Eyes on the Street [43] and Newman’s Defensible Space Theory [46].

Our study also underscores the ethical implications of using LMMs for urban safety classification. The significant variation in unsafe classifications across socio-demographic Personas suggests that LMMs may inadvertently amplify societal biases. If AI-driven safety assessments are deployed without explicitly considering whose perspective is being represented, they risk privileging certain viewpoints while marginalizing others. Thus, from an AI ethics perspective, these findings highlight the necessity of transparency in model training datasets and deployment, ensuring that stakeholders understand how LMMs classify safety, what biases they encode, and how their outputs should be interpreted.

While our study provides valuable insights into the application of LMMs for urban safety perception, it is important to acknowledge also the limitations. First, our analysis was conducted using a single multimodal model (Llava 1.6 7B). Future work should evaluate multiple models to assess whether observed biases are specific to Llava or if they generalize across other vision-language architectures. Second, while we employed socio-demographic Personas to probe biases, our approach remains constrained by the limited number of demographic attributes tested. Future studies should explore intersectional biases (e.g., combining gender, age, and nationality), to examine how multiple identity factors interact in shaping safety perceptions, and take into account a wider number of socio-demographic variables (e.g., considering all the nationalities).

This study highlights the potential of LMMs for urban safety perception. Their ability to classify urban scenarios

offers a scalable, cost-effective alternative to traditional methods, such as surveys, which are time-intensive and often outdated. Moreover, through several analyses of the model’s output, we identified the underlying factors driving its classifications, offering valuable insights to inform decision-making for policymakers and urban planners. However, the results also underscore the ethical and practical challenges of deploying such models in real-world applications. Future work should focus on bias mitigation, dataset diversification, and multi-model validation to ensure that AI-driven urban assessments are both fair and reliable. By addressing these challenges, we can leverage LMMs to augment traditional urban planning methodologies while safeguarding against the unintended amplification of societal biases.

MATERIALS AND METHODS

Dataset

For our analysis, we employed the Place Pulse 2.0 dataset [15], a crowd-sourced collection of urban perception data covering 56 cities across six continents. The dataset was created by asking online volunteers to compare pairs of images and choose which one looks "safer", "livelier", "more boring", "wealthier", "more depressing", or "more beautiful", collecting over 1,169,078 pairwise comparisons for the 110,988 images contained. The images were carefully chosen using a uniform grid based on latitude and longitude to ensure the representation of each city’s districts, spanning the years 2007 to 2012. User preferences have been converted to image-level ranks of safeness perception between 0 and 5 using the Trueskill algorithm [58]. The TrueSkill algorithm, originally developed by Microsoft Research for ranking players in multiplayer games, offers a robust framework for converting subjective pairwise comparisons into objective ratings. In urban perception studies [13], this algorithm is applied to street-level imagery where participants compare images based on attributes like safety, liveliness, and other urban qualities. Each image is initially modelled as a Gaussian distribution characterized by a mean (an initial estimate of its perceived quality) and a variance (indicating the uncertainty about that estimate). When two images are compared, the outcome is used to update both images’ distributions through Bayesian inference. This process adjusts the mean, thereby refining the estimate of an image’s quality, and reduces the variance, reflecting increased confidence in the rating. As more pairwise comparisons are processed, the iterative updates lead to stable and reliable rankings. Additional details on how votes are converted into scores can be found in [13]. In Supplementary Note S6 and Supplementary Table S10, we show additional information on the original dataset, like the spatial distribution of the images and the distribution of the safeness scores.

In our experiments, we perform a binary classification task, asking the model to classify images as *Safe* or *Unsafe*. Thus, we convert the scores associated with the images to labels. In the main paper, we label the images as unsafe if their scores are lower than or equal to the average of the scores (0.464). Otherwise, we consider them safe.

Models

In our work, we leverage Llava 1.6 7B [41, 42]. Despite reducing the temperature to 0.1 to ensure a better reproducibility of our study, we keep the default parameters. We deployed a Llava instance on an 11 GB RTX 2080, and each image’s response is provided, on average, in 2.9 seconds.

Technically, Llava is a large multimodal model trained end-to-end. It combines a CLIP ViT-L/14 [59] vision encoder and the large language model Vicuna [60] for vision-language understanding. The two encoders are connected with a projection matrix. The model is then trained using a two-stage instruction-tuning procedure. Additional details on the model’s training and performances can be found in [41, 42]

Evaluation Metrics

1. Thresholding and Ground Truth

To establish a classification framework for urban safety perception, we normalize the original `TrueSkill score` from the Place Pulse 2.0 dataset to ensure comparability across images. Given an image i , its normalized TrueSkill score is computed as:

$$\text{trueskill_normalized}_i = \frac{\text{TrueSkill score}_i - \min(\text{TrueSkill score})}{\max(\text{TrueSkill score}) - \min(\text{TrueSkill score})}.$$

Using this normalized scale, we define a threshold τ to distinguish between *Safe* and *Unsafe* classifications. We adopt an adaptive approach where the threshold is set to the mean of the normalized TrueSkill scores:

$$\tau = \text{mean}(\text{trueskill_normalized}).$$

With this threshold ($\tau = 0.464$), each image is classified into one of the two categories based on its normalized safety perception score:

$$\text{True_Ground}_i = \begin{cases} \text{Safe}, & \text{if } \text{trueskill_normalized}_i > \tau, \\ \text{Unsafe}, & \text{otherwise.} \end{cases}$$

This adaptive thresholding ensures that safety classifications reflect the relative perception of urban environments

within the dataset rather than an arbitrary fixed boundary.

2. Classification Metrics

We employ standard classification metrics to evaluate the model’s performance based on the number of correctly and incorrectly predicted *Safe* and *Unsafe* labels. Specifically, we define True Positive (TP) as the number of images correctly predicted as Safe, and True Negative (TN) as the number of images correctly predicted as Unsafe. False Positive (FP) is defined as the number of Unsafe images misclassified as Safe, while False Negative (FN) is the number of Safe images misclassified as Unsafe.

We then compute Precision, Recall, and the F1-score. Precision, which measures the proportion of correctly predicted Safe images among all images classified as Safe, is given by:

$$\text{Precision} = \frac{TP}{TP + FP}.$$

Recall, which captures the proportion of correctly predicted Safe images among all truly Safe images, is computed as:

$$\text{Recall} = \frac{TP}{TP + FN}.$$

To balance Precision and Recall, we calculate the F1-score as their harmonic mean:

$$\text{F1-score} = 2 \cdot \frac{\text{Precision} \times \text{Recall}}{\text{Precision} + \text{Recall}}.$$

Additionally, for each prompt, we quantify the proportion of images classified as *Unsafe* by the model:

$$\text{UNSAFE N. (\%)} = \frac{\text{number of Unsafe classified predictions}}{\text{total number of images}} \times 100.$$

This metric provides insights into how frequently different prompts lead the model to classify urban spaces as Unsafe, offering a comparative measure across the different prompts used.

3. Rank Correlations of City Ordering

To analyze the consistency in the model’s classification of unsafe environments across different prompts, we assess the correlation between city rankings using Spearman’s rank correlation coefficient ρ . This non-parametric measure evaluates the degree to which two rankings follow the same order, capturing both the strength and direction of association. Given the ranks of cities under two different prompts, the Spearman correlation is computed as:

$$\rho = 1 - \frac{6 \sum d_i^2}{n(n^2 - 1)},$$

where d_i represents the difference in ranks for city i across two rankings, and n is the number of cities. This approach allows us to determine the extent to which different nationalities or perspectives lead to consistent or diverging perceptions of urban safety.

4. Hierarchical Clustering

To further explore patterns in urban safety perception, we apply hierarchical clustering to group both *cities* and *nationalities* based on their mean proportion of *Unsafe* classifications. For nationalities, we also incorporate the standard deviation of their unsafe classifications to capture variability for each nationality across each city.

The clustering process consists of several key steps. First, we compute the pairwise dissimilarity between data points using the Euclidean distance, defined as:

$$d(x, y) = \sqrt{\sum_{i=1}^n (x_i - y_i)^2},$$

where x and y are data points representing either cities or nationalities. Next, we determine the *linkage criterion*, which defines how distances between clusters are measured. We employ Ward’s method [61], which minimizes the total within-cluster variance at each step. The distance between two clusters A and B is given by:

$$d(A, B) = \sqrt{\frac{|A||B|}{|A| + |B|} \|c_A - c_B\|^2},$$

where $|A|$ and $|B|$ denote the sizes of clusters A and B , and c_A and c_B are their respective centroids.

A *dendrogram* is then constructed to visualize the hierarchical structure, illustrating how clusters are merged at successive steps. The height of each branch represents the dissimilarity between merged clusters, providing a clear

depiction of relationships between groups. Finally, we determine the optimal number of clusters by applying a threshold to the dendrogram, ensuring a balance between granularity and interpretability.

5. Comparison with the Neutral Prompt

To assess how different prompts influence the model’s safety classifications, we compare each prompt’s tendency to label images as *Unsafe* against the *Neutral prompt* baseline. Specifically, we measure the change in the proportion of images classified as *Unsafe* for each city under a given prompt.

Let $\text{UNSAFE_mean}(p, c)$ be the average fraction (%) of images classified as *Unsafe* under prompt p . Likewise, let $\text{UNSAFE_mean}(\text{Neutral}, c)$ be that city’s unsafe classification rate under the *Neutral* prompt. We define the city-level difference as follows:

$$\Delta_{\text{Unsafe}}(p, c) = \text{UNSAFE_mean}(p, c) - \text{UNSAFE_mean}(\text{Neutral}, c). \quad (1)$$

A positive $\Delta_{\text{Unsafe}}(p, c)$ indicates that prompt p yields a higher unsafe rate than the neutral baseline in city c .

We further compute a single summary value for prompt p by averaging across all N cities:

$$\Delta_{\text{Unsafe}}(p) = \frac{1}{N} \sum_{c=1}^N \Delta_{\text{Unsafe}}(p, c), \quad (2)$$

Further, to assess the alignment of socio-demographic prompts p with the *Neutral* baseline, we compute the percentage of predictions that match the classification of the *Neutral* prompt, treating the latter as a “ground truth” reference. Concretely, let I be the set of images evaluated under both the neutral configuration and a particular prompt p . We then define:

$$\text{Accuracy}(p) = \frac{1}{|I|} \sum_{i \in I} \mathbf{1}(\text{cls}_p(i) = \text{cls}_{\text{Neutral}}(i)),$$

where $\text{cls}_p(i)$ is the label assigned by prompt p to image i , and $\text{cls}_{\text{Neutral}}(i)$ is the neutral prompt’s classification of the same image. The indicator function $\mathbf{1}(\cdot)$ evaluates to 1 if both classifications match and 0 otherwise.

6. Keyword Network Construction and Community Detection

a. Keyword Extraction and Normalization. We focus exclusively on images classified as *Unsafe*. For each such image, we collect the set of descriptive keywords $\{k_1, k_2, \dots, k_n\}$. To standardize these keywords, we apply a normalization procedure that removes punctuation, converts text to lowercase, and maps known synonyms (e.g., “vehicle traffic” to “traffic”) to a single canonical form. We define the normalized version of a raw keyword k as:

$$\hat{k} = \mathcal{N}(k),$$

where $\mathcal{N}(\cdot)$ represents the normalization function. This transformation ensures that semantically equivalent terms are treated consistently throughout the analysis.

$$\hat{k} = \mathcal{N}(k)$$

denote the normalized version of a raw keyword k , where $\mathcal{N}(\cdot)$ is the normalization function.

b. Co-occurrence Matrix. To build the network, we select the top N most frequent keywords in the dataset of Unsafe images. Denote this reduced set by $\mathcal{K} = \{\kappa_1, \kappa_2, \dots, \kappa_N\}$. For each image i , let $\mathcal{K}_i \subseteq \mathcal{K}$ be the subset of top- N normalized keywords present in that image. We then construct an $N \times N$ co-occurrence matrix \mathbf{A} , where

$$A_{mn} = \sum_{i=1}^M \mathbf{1}(\{\kappa_m, \kappa_n\} \subseteq \mathcal{K}_i),$$

for $1 \leq m, n \leq N$. Here, $\mathbf{1}(\cdot)$ is an indicator function that is 1 if both keywords κ_m and κ_n appear together in image i , and 0 otherwise. Consequently, A_{mn} measures the number of images where the two keywords co-occur.

c. Network Representation. We interpret \mathbf{A} as the adjacency matrix of an undirected graph $G = (V, E)$, in which V is the set of keywords (nodes) and E the set of edges. An edge between κ_m and κ_n exists if $A_{mn} > 0$, with the edge weight $w_{mn} = A_{mn}$.

d. Community Detection via Louvain. To identify thematic groupings of keywords, we apply the *Louvain* method to detect communities in the network G [62]. The Louvain algorithm optimizes the modularity Q , defined as

$$Q = \frac{1}{2W} \sum_{(m,n) \in E} \left[w_{mn} - \frac{d_m d_n}{2W} \right] \delta(\gamma_m, \gamma_n),$$

where $d_m = \sum_n w_{mn}$ is the weighted degree of node m , $W = \frac{1}{2} \sum_{m,n} w_{mn}$ is the sum of all edge weights, $\delta(\gamma_m, \gamma_n)$ is 1 if nodes m and n share the same community label, and 0 otherwise.

e. Degree Centrality. Once each community is identified, we compute a node's *degree centrality* relative to its own community. For a community $C \subseteq V$ and a node $v \in C$, define:

$$\text{DC}_C(v) = \frac{\deg_C(v)}{|C| - 1},$$

where $\deg_C(v)$ is the degree of v within C . Nodes with higher $\text{DC}_C(v)$ in a community appear most frequently in co-occurrence with other community members, suggesting they represent key thematic elements.

Prompt

In this study, we employed a series of carefully structured prompts to test the model’s assessment of urban safety, with the *Neutral prompt* serving as the foundational baseline. This baseline scenario, shown in Table I, avoids specifying any socio-demographic context and instructs the model to classify scenes as *Safe* or *Unsafe* solely based on visible evidence. To ensure balance in uncertain scenarios, we adopted a conservative stance, defaulting to *Unsafe* when the evidence is ambiguous. Furthermore, the required output is structured as a JSON object, containing the classification, three descriptive keywords, and a reason for the decision.

Neutral Prompt

Your task is to classify the area in the image as "Safe" or "Unsafe" based on visible indicators of security, safety, and livability from an individual perspective.

Avoid assuming safety unless there is clear, strong, and visible evidence supporting a "Safe" classification. If prominent risks are observed, prioritize these concerns in your assessment and lean towards an "Unsafe" classification. Also, consider the cumulative impact of multiple negative indicators on the overall perception of safety.

Provide your classification along with 3 specific keywords and a reason that accurately reflect the observed evidence justifying your choice. Organize your response in a JSON object with the following keys:

```
{
  "Classification": (your answer),
  "Keywords": (the 3 keywords),
  "Reason": (sentence that explains your choices)
}
```

Table I. Neutral Prompt used in the study. Baseline scenario with no explicit socio-demographic references.

Building on this foundation, we introduced a variety of prompts that incorporate specific socio-demographic perspectives, enhancing the model’s sensitivity to diverse Personas. It is worth noticing that the core structure of all the prompts remains the same, to enhance the comparability of the results. The only relevant variation lies in the opening sentence, which specifies the perspective the model is instructed to adopt. The whole prompts are provided in Supplementary Note S4, Supplementary Table S4-S6. Below, we summarize their key characteristics:

- **Nationality Prompts:** Configured to reflect the perspective of individuals from one of 32 nationalities represented in the Place Pulse 2.0 dataset, these prompts allow us to examine how cultural backgrounds may influence the model’s safety assessments, ensuring they are pertinent to the respective urban environments.
- **Age Prompts:** Divided into *Young*, *Middle*, and *Eldery*, these prompts adjust the model to consider safety from the viewpoint of different life stages, acknowledging the variability in perceived risks or safety across generations.

- **Gender Prompts:** Comprising *Male* and *Female*, these prompts enable the model to consider how safety perceptions may vary based on gender-specific experiences.

This approach not only provides the model with a broad spectrum of perspectives but also allows for a detailed examination of how specific demographic or cultural frames influence features commonly associated with safety perceptions in urban scenarios. By keeping the output requirements consistent and the semantic structure uniform across all prompts, we can compare variations in the model’s perception of urban safety with precision.

ACKNOWLEDGMENTS

B.L. has been supported by PRECRISIS (PRotECTing public spaces thRough Integrated Smarter Innovative Security) is funded by the European Union Internal Security Fund (ISFP-2022-TFI-AG-PROTECT-02-101100539). B.L. and M.L. has been supported by the PNRR ICSC National Research Centre for High Performance Computing, Big Data and Quantum Computing (CN00000013), under the NRRP MUR program funded by the NextGenerationEU. B.L. also acknowledges the support of the PNRR project FAIR - Future AI Research (PE00000013), under the NRRP MUR program funded by the NextGenerationEU and by the European Union’s Horizon Europe research and innovation program under grant agreement No. 101120237 (ELIAS). Portions of the paper were developed from the thesis of S.B.

Contributions

C.B. designed and developed the model. C.B. performed the experiments. M.L. designed the study. C.B., B.L and M.L. contributed to interpreting the results and writing the paper. M.L. coordinated the writing of the paper.

Competing Financial Interests

The authors declare no competing financial interests

Data Availability

The data used in this work are publicly available from the original references

Code Availability

The code to perform the analysis will be available upon request.

-
- [1] M. Carmona, Contemporary public space: Critique and classification, part one: Critique, *Journal of urban design* **15**, 123 (2010).
 - [2] M. Luca, B. Lepri, R. Gallotti, S. Paolazzi, M. Bigi, and M. Pistore, Towards civic digital twins: Co-design the citizen-centric future of bologna, *arXiv preprint arXiv:2412.06328* (2024).
 - [3] C. Ahn, F. Lotfi-Jam, C. Graham, T. Bunnell, and S. Marvin, Critical urban informatics for urban digital twin models, *Nature Cities* 10.1038/s44284-024-00171-0 (2025).
 - [4] P. Saleses, K. Schechtner, and C. A. Hidalgo, The collaborative image of the city: mapping the inequality of urban perception, *PloS one* **8**, e68400 (2013).
 - [5] H. Zamanifard, T. Alizadeh, C. Bosman, and E. Coiacetto, Measuring experiential qualities of urban public spaces: users' perspective, *Journal of Urban Design* **24**, 340 (2019).
 - [6] V. Mehta, Evaluating public space, *Journal of Urban design* **19**, 53 (2014).
 - [7] F. Simini, G. Barlacchi, M. Luca, and L. Pappalardo, A deep gravity model for mobility flows generation, *Nature communications* **12**, 6576 (2021).
 - [8] M. Bahrami, Y. Xu, M. Tweed, B. Bozkaya, *et al.*, Using gravity model to make store closing decisions: A data driven approach, *Expert systems with applications* **205**, 117703 (2022).
 - [9] Y. Suhara, M. Bahrami, B. Bozkaya, and A. S. Pentland, Validating gravity-based market share models using large-scale transactional data, *Big Data* **9**, 188 (2021).
 - [10] T. Gebru, J. Krause, Y. Wang, D. Chen, J. Deng, E. L. Aiden, and L. Fei-Fei, Using deep learning and google street view to estimate the demographic makeup of neighborhoods across the united states, *Proceedings of the National Academy of Sciences* **114**, 13108–13113 (2017).
 - [11] M. Helbich, Y. Yao, Y. Liu, J. Zhang, P. Liu, and R. Wang, Using deep learning to examine street view green and blue spaces and their associations with geriatric depression in beijing, china, *Environment International* **126**, 107 (2019).
 - [12] Y.-H. Ho, L. Li, and A. Mostafavi, Elev-vision-sam: Integrated vision language and foundation model for automated estimation of building lowest floor elevation (2024), *arXiv:2404.12606 [cs.CV]*.
 - [13] N. Naik, J. Philipoom, R. Raskar, and C. Hidalgo, Streetscore-predicting the perceived safety of one million streetscapes, in *Proceedings of the IEEE conference on computer vision and pattern recognition workshops* (2014) pp. 779–785.
 - [14] M. De Nadai, R. L. Vieriu, G. Zen, S. Dragicevic, N. Naik, M. Caraviello, C. A. Hidalgo, N. Sebe, and B. Lepri, Are safer looking neighborhoods more lively? a multimodal investigation into urban life, in *Proceedings of the 24th ACM international conference on Multimedia* (2016) pp. 1127–1135.
 - [15] A. Dubey, N. Naik, D. Parikh, R. Raskar, and C. A. Hidalgo, Deep learning the city : Quantifying urban perception at a global scale (2016), *arXiv:1608.01769 [cs.CV]*.

- [16] M. Redi, L. M. Aiello, R. Schifanella, and D. Quercia, The spirit of the city: Using social media to capture neighborhood ambiance, *Proceedings of the ACM on human-computer interaction* **2**, 1 (2018).
- [17] D. Quercia, N. K. O’Hare, and H. Cramer, Aesthetic capital: what makes london look beautiful, quiet, and happy?, in *Proceedings of the 17th ACM conference on Computer supported cooperative work & social computing* (2014) pp. 945–955.
- [18] Y. Hou, M. Quintana, M. Khomiakov, W. Yap, J. Ouyang, K. Ito, Z. Wang, T. Zhao, and F. Biljecki, Global streetscapes—a comprehensive dataset of 10 million street-level images across 688 cities for urban science and analytics, *ISPRS Journal of Photogrammetry and Remote Sensing* **215**, 216 (2024).
- [19] A. Dubey, N. Naik, D. Parikh, R. Raskar, and C. A. Hidalgo, Deep learning the city: Quantifying urban perception at a global scale, in *Computer Vision—ECCV 2016: 14th European Conference, Amsterdam, The Netherlands, October 11–14, 2016, Proceedings, Part I 14* (Springer, 2016) pp. 196–212.
- [20] P. E. Gustafson, Gender differences in risk perception: Theoretical and methodological perspectives, *Risk analysis* **18**, 805 (1998).
- [21] M. Raudsepp, Some socio-demographic and socio-psychological predictors of environmentalism, *Trames* **5**, 355 (2001).
- [22] S. Dlamini, S. G. Tesfamichael, Y. Shiferaw, and T. Mokhele, Determinants of environmental perceptions and attitudes in a socio-demographically diverse urban setup: The case of gauteng province, south africa, *Sustainability* **12**, 3613 (2020).
- [23] S.-J. Park, S. Choi, and E.-J. Kim, The relationships between socio-demographic variables and concerns about environmental sustainability, *Corporate Social Responsibility and Environmental Management* **19**, 343 (2012).
- [24] A. K. Christian, B. D. Dovie, W. Akpalu, and S. N. A. Codjoe, Households’ socio-demographic characteristics, perceived and underestimated vulnerability to floods and related risk reduction in ghana, *Urban Climate* **35**, 100759 (2021).
- [25] B. Sharma and D. Gursoy, An examination of changes in residents’ perceptions of tourism impacts over time: The impact of residents’ socio-demographic characteristics, *Asia Pacific Journal of Tourism Research* **20**, 1332 (2015).
- [26] I. Stojković, J. Tepavčević, I. Blešić, M. Ivkov, and V. Šimon, Influence of sociodemographic characteristics on perception of tourism development impact, *The European Journal of Applied Economics* **17** (2020).
- [27] M. L. Finucane, P. Slovic, C. K. Mertz, J. Flynn, and T. Satterfield, Gender, race and perceived risk: The ‘white-male’ effect, in *The Feeling of Risk* (Routledge, 2013) pp. 125–139.
- [28] A. Olofsson and S. Rashid, The white (male) effect and risk perception: can equality make a difference?, *Risk Analysis: An International Journal* **31**, 1016 (2011).
- [29] S. Niforatos, D. Panagiotakos, and P.-M. Delladetsimas, Socio-demographic determinants of earthquake risk perception: the case of the corinthiakos gulf, in greece, *Natural Hazards* **120**, 3847 (2024).
- [30] A. Phillips, A. Z. Khan, and F. Canters, Use-related and socio-demographic variations in urban green space preferences, *Sustainability* **13**, 3461 (2021).
- [31] L. C. Hui and C. Y. Jim, Urban-greenery demands are affected by perceptions of ecosystem services and disservices, and socio-demographic and environmental-cultural factors, *Land Use Policy* **120**, 106254 (2022).
- [32] Z. Fan, F. Zhang, B. P. Loo, and C. Ratti, Urban visual intelligence: Uncovering hidden city profiles with street view images, *Proceedings of the National Academy of Sciences* **120**, e2220417120 (2023).
- [33] H. Liu, C. Li, Y. Li, and Y. J. Lee, Improved baselines with visual instruction tuning (2023).
- [34] H. Liu, C. Li, Q. Wu, and Y. J. Lee, Visual instruction tuning (2023).

- [35] P. Hämäläinen, M. Tavast, and A. Kunnari, Evaluating large language models in generating synthetic hci research data: a case study, in *Proceedings of the 2023 CHI Conference on Human Factors in Computing Systems* (2023) pp. 1–19.
- [36] J. S. Park, J. O’Brien, C. J. Cai, M. R. Morris, P. Liang, and M. S. Bernstein, Generative agents: Interactive simulacra of human behavior, in *Proceedings of the 36th annual acm symposium on user interface software and technology* (2023) pp. 1–22.
- [37] E. Fleisig, R. Abebe, and D. Klein, When the majority is wrong: Modeling annotator disagreement for subjective tasks, arXiv preprint arXiv:2305.06626 (2023).
- [38] J. J. Horton, *Large language models as simulated economic agents: What can we learn from homo silicus?*, Tech. Rep. (National Bureau of Economic Research, 2023).
- [39] L. P. Argyle, E. C. Busby, N. Fulda, J. R. Gubler, C. Rytting, and D. Wingate, Out of one, many: Using language models to simulate human samples, *Political Analysis* **31**, 337 (2023).
- [40] P. Törnberg, D. Valeeva, J. Uitermark, and C. Bail, Simulating social media using large language models to evaluate alternative news feed algorithms, arXiv preprint arXiv:2310.05984 (2023).
- [41] H. Liu, C. Li, Q. Wu, and Y. J. Lee, Visual instruction tuning, *Advances in neural information processing systems* **36** (2024).
- [42] H. Liu, C. Li, Y. Li, and Y. J. Lee, Improved baselines with visual instruction tuning, in *Proceedings of the IEEE/CVF Conference on Computer Vision and Pattern Recognition* (2024) pp. 26296–26306.
- [43] J. Jacobs, *The Death and Life of Great American Cities* (Knopf Doubleday Publishing Group, 1992).
- [44] G. L. Kelling and J. Q. Wilson, Broken windows: The police and neighborhood safety, *The Atlantic* (1982).
- [45] P. Branco, L. Torgo, and R. P. Ribeiro, A survey of predictive modeling on imbalanced domains, *ACM computing surveys (CSUR)* **49**, 1 (2016).
- [46] O. Newman, *Defensible Space; Crime Prevention Through Urban Design*, Architecture/Urban affairs (Macmillan, 1972).
- [47] C. Shaw and H. McKay, *Juvenile Delinquency and Urban Areas: A Study of Rates of Delinquents in Relation to Differential Characteristics of Local Communities in American Cities*, Behavior research fund monographs (University of Chicago Press, 1942).
- [48] R. J. Sampson and W. B. Groves, Community structure and crime: Testing social-disorganization theory, *American journal of sociology* **94**, 774 (1989).
- [49] C. Beneduce, B. Lepri, and M. Luca, Large language models are zero-shot next location predictors (2024), arXiv:2405.20962 [cs.CY].
- [50] J. Li, C. Liu, S. Cheng, R. Arcucci, and S. Hong, Frozen language model helps ecg zero-shot learning (2023), arXiv:2303.12311 [cs.LG].
- [51] N. Gruver, M. Finzi, S. Qiu, and A. G. Wilson, Large language models are zero-shot time series forecasters (2024), arXiv:2310.07820 [cs.LG].
- [52] J. Forester, *The Deliberative Practitioner: Encouraging Participatory Planning Processes*, Mit Press (MIT Press, 1999).
- [53] P. Healey, *Collaborative Planning: Shaping Places in Fragmented Societies*, Canadian electronic library: Books collection (UBC Press, 1997).

- [54] J. Wei, X. Wang, D. Schuurmans, M. Bosma, B. Ichter, F. Xia, E. Chi, Q. Le, and D. Zhou, Chain-of-thought prompting elicits reasoning in large language models (2023), arXiv:2201.11903 [cs.CL].
- [55] R. Bommasani, D. A. Hudson, E. Adeli, R. Altman, S. Arora, S. von Arx, M. S. Bernstein, J. Bohg, A. Bosselut, E. Brunskill, E. Brynjolfsson, S. Buch, D. Card, R. Castellon, N. Chatterji, A. Chen, K. Creel, J. Q. Davis, D. Demszky, C. Donahue, M. Doumbouya, E. Durmus, S. Ermon, J. Etchemendy, K. Ethayarajh, L. Fei-Fei, C. Finn, T. Gale, L. Gillespie, K. Goel, N. Goodman, S. Grossman, N. Guha, T. Hashimoto, P. Henderson, J. Hewitt, D. E. Ho, J. Hong, K. Hsu, J. Huang, T. Icard, S. Jain, D. Jurafsky, P. Kalluri, S. Karamcheti, G. Keeling, F. Khani, O. Khattab, P. W. Koh, M. Krass, R. Krishna, R. Kuditipudi, A. Kumar, F. Ladhak, M. Lee, T. Lee, J. Leskovec, I. Levent, X. L. Li, X. Li, T. Ma, A. Malik, C. D. Manning, S. Mirchandani, E. Mitchell, Z. Munyikwa, S. Nair, A. Narayan, D. Narayanan, B. Newman, A. Nie, J. C. Niebles, H. Nilforoshan, J. Nyarko, G. Ogut, L. Orr, I. Papadimitriou, J. S. Park, C. Piech, E. Portelance, C. Potts, A. Raghunathan, R. Reich, H. Ren, F. Rong, Y. Roohani, C. Ruiz, J. Ryan, C. Ré, D. Sadigh, S. Sagawa, K. Santhanam, A. Shih, K. Srinivasan, A. Tamkin, R. Taori, A. W. Thomas, F. Tramèr, R. E. Wang, W. Wang, B. Wu, J. Wu, Y. Wu, S. M. Xie, M. Yasunaga, J. You, M. Zaharia, M. Zhang, T. Zhang, X. Zhang, Y. Zhang, L. Zheng, K. Zhou, and P. Liang, On the opportunities and risks of foundation models (2022), arXiv:2108.07258 [cs.LG].
- [56] S. Longpre, N. Singh, M. Cherep, K. Tiwary, J. Materzynska, W. Brannon, R. Mahari, M. Dey, M. Hamdy, N. Saxena, *et al.*, Bridging the data provenance gap across text, speech and video, arXiv preprint arXiv:2412.17847 (2024).
- [57] S. T. Fiske, Stereotype content: Warmth and competence endure, *Current Directions in Psychological Science* **27**, 67 (2018), PMID: 29755213, <https://doi.org/10.1177/0963721417738825>.
- [58] R. Herbrich, T. Minka, and T. Graepel, Trueskill™: a bayesian skill rating system, *Advances in neural information processing systems* **19** (2006).
- [59] A. Radford, J. W. Kim, C. Hallacy, A. Ramesh, G. Goh, S. Agarwal, G. Sastry, A. Askell, P. Mishkin, J. Clark, *et al.*, Learning transferable visual models from natural language supervision, in *International conference on machine learning* (PMLR, 2021) pp. 8748–8763.
- [60] W.-L. Chiang, Z. Li, Z. Lin, Y. Sheng, Z. Wu, H. Zhang, L. Zheng, S. Zhuang, Y. Zhuang, J. E. Gonzalez, I. Stoica, and E. P. Xing, Vicuna: An open-source chatbot impressing gpt-4 with 90%* chatgpt quality (2023).
- [61] J. H. Ward Jr, Hierarchical grouping to optimize an objective function, *Journal of the American statistical association* **58**, 236 (1963).
- [62] M. Newman, *Networks: An Introduction* (OUP Oxford, 2010).

Supplementary Information for Urban Safety Perception Through the Lens of Large Multimodal Models: A Persona-based Approach

S1. NEUTRAL PROMPT

In this section, we present the evaluation of the **Neutral Prompt**, a prompt designed to assess safety perception without incorporating socio-demographic biases. The goal of this prompt is to determine whether an area is classified as *Safe* or *Unsafe* based purely on visual indicators of security, infrastructure, and urban livability.

Unlike prompts that explicitly condition responses on personal attributes such as nationality, gender, or age, the Neutral Prompt aims to establish a baseline classification. This allows us to analyze the inherent tendencies of the model when assessing urban safety without external contextual framing.

To evaluate the model’s classification performance under the Neutral Prompt, we compute the **F1-score**, **precision**, and **recall** for each city. These metrics are averaged over two experimental runs to ensure robustness. Table S1 summarizes the results, including the mean and standard deviation of F1-scores per city.

Table S1. F1-score per city, and with precision, recall and standard deviation, for the Neutral Prompt across the 2 runs.

City	F1 Score (Mean)	Precision (Mean)	Recall (Mean)	F1 Score (Std)
Minneapolis	72.317	60.600	89.650	0.354
Denver	71.184	58.600	90.650	0.141
Toronto	70.288	57.700	89.900	0.283
WashingtonDC	69.965	57.450	89.450	0.707
Portland	69.841	57.000	90.150	0.212
Atlanta	69.411	57.650	87.200	0.283
Boston	69.000	56.200	89.350	0.283
Montreal	68.274	56.650	85.900	0.071
CapeTown	68.045	58.250	81.800	0.495
Sydney	67.560	56.300	84.450	0.283
Dublin	67.443	57.850	80.850	0.071
Seattle	67.254	54.500	87.800	0.212
Munich	66.695	59.450	75.950	0.424
Amsterdam	66.070	58.200	76.400	0.354
Prague	65.663	59.600	73.100	0.212
Chicago	65.642	56.250	78.800	0.354
SanFrancisco	65.638	53.700	84.400	0.141
Berlin	65.352	57.350	75.950	0.141
Melbourne	65.314	55.400	79.550	0.141
Madrid	64.890	57.900	73.800	0.495
Helsinki	64.802	55.500	77.850	0.283
LosAngeles	64.685	53.450	81.900	0.071
Warsaw	64.598	58.250	72.500	0.354
Singapore	64.349	59.150	70.550	0.071
Johannesburg	64.151	56.500	74.200	0.212
Bratislava	63.892	57.050	72.600	0.283
Houston	62.892	57.500	69.400	0.424
Copenhagen	62.780	54.900	73.300	2.121
Stockholm	62.650	54.000	74.600	0.354
Paris	62.566	52.950	76.450	0.141
NewYork	62.387	52.600	76.650	0.495
London	62.347	56.300	69.850	0.283
Philadelphia	61.955	53.950	72.750	0.212
Glasgow	61.714	57.950	66.000	0.000
Milan	61.522	55.250	69.400	0.071
Barcelona	61.440	55.900	68.200	0.071
Kyoto	60.821	57.700	64.300	0.707
Lisbon	59.374	54.750	64.850	0.495
Rome	59.220	55.750	63.150	0.424
TelAviv	58.757	52.850	66.150	1.131
Zagreb	58.349	57.150	59.600	0.283
Tokyo	57.616	55.500	59.900	0.212
Santiago	57.157	52.550	62.650	0.212
Guadalajara	56.291	53.450	59.450	0.354
Gaborone	54.966	57.200	52.900	0.919
Bucharest	52.910	54.400	51.500	0.424
Moscow	47.388	55.400	41.400	0.354
Valparaiso	46.575	46.700	46.450	0.990
MexicoCity	45.009	48.350	42.100	0.141
Kiev	42.358	54.600	34.600	0.424
HongKong	38.643	51.150	31.050	0.071
SaoPaulo	35.341	51.500	26.900	0.071
BeloHorizonte	31.502	51.200	22.750	0.000
Bangkok	31.179	54.100	21.900	0.212
Taipei	30.378	54.550	21.050	0.212
RioDeJaneiro	27.363	50.250	18.800	0.141

S2. HIERARCHICAL CLUSTERING

S3. KEYWORD NETWORK AND COMMUNITY DETECTION

To understand the underlying reasons driving safety classifications, we analyzed the most frequently occurring keywords in the responses. Using network analysis and community detection techniques, we identified clusters of related terms associated with *Safe* and *Unsafe* classifications.

Tables S2 and S3 report the identified communities, sorted by degree centrality, which quantifies the relative importance of each term within its community.

Table S2. Safe Network Communities Sorted by Degree Centralities

Community	Term	Degree Centrality
Community 0		
	neighborhood	1.0000
	residential	1.0000
	trees	1.0000
	parking	0.8750
	security	0.8750
	street	0.8750
	parked cars	0.7500
	safety	0.7500
	peaceful	0.6250
Community 1		
	orderly	1.0000
	residential area	1.0000
	secure	1.0000
	wellmaintained	1.0000
	empty	0.8889
	quiet	0.8889
	rural	0.8889
	low crime	0.7778
	no visible threats	0.7778
	accessible	0.4444
Community 2		
	commercial	1.0000
	infrastructure	1.0000
	traffic	1.0000
	urban	1.0000
	vehicles	1.0000

Table S3. Unsafe Network Communities Sorted by Degree Centralities

Community	Term	Degree Centrality
Community 0		
	abandoned	1.0000
	dilapidated	1.0000
	isolated	1.0000
	neglected	1.0000
	graffiti	0.8750
	vacant	0.8750
	insecure	0.7500
	rural	0.7500
	vandalism	0.7500
Community 1		
	empty	1.0000
	security concerns	1.0000
	lack of maintenance	0.8750
	potential for crime	0.8750
	deserted	0.7500
	gated community	0.7500
	lack of pedestrians	0.7500
	parked cars	0.7500
	rundown	0.7500
Community 2		
	fence	1.0000
	infrastructure	1.0000
	parking	1.0000
	security	1.0000
	traffic	1.0000
	urban	1.0000
	vehicles	1.0000

S4. PROMPTS COMPARISON

A. Overview

Understanding how urban safety perception varies across different socio-demographic groups requires a well-structured prompting strategy. In this section, we detail three distinct prompts used to evaluate safety classification from different perspectives: nationality, gender, and age.

The prompts are designed to:

- Encourage the model to consider cultural, gender-based, and age-related factors in safety perception.
- Ensure consistency by using a structured JSON output format and minor changes across prompts.

The detailed prompt structures are presented in Tables S4, S5, and S6.

B. Prompts Structure

Nationality Prompt
<p>Assume the role of a person born and raised in <Country>. Your task is to classify the area in the image as "Safe" or "Unsafe" based on visible indicators of security, safety, and livability from the perspective of someone of your nationality.</p> <p>Avoid assuming safety unless there is clear, strong, and visible evidence supporting a "Safe" classification. If prominent risks are observed, prioritize these concerns in your assessment and lean towards an "Unsafe" classification. Consider how someone from your nationality would perceive the area. Also, consider the cumulative impact of multiple negative indicators on the overall perception of safety.</p> <p>Provide your classification along with 3 specific keywords and a reason that accurately reflects the observed evidence justifying your choice. Organize your response in a JSON object with the following keys:</p> <pre>{ "Classification": (your answer) "Keywords": (the 3 keywords) "Reason": (sentence that explains your choices) }</pre>

Table S4. The Nationality Prompt, illustrating how the model is instructed to assume a cultural perspective when assessing urban safety. This base prompt includes a <Country> placeholder, which is iteratively substituted by one of the 32 nations from the Place Pulse 2.0 dataset.

Gender Prompt

Assume the role of a male/female person. Your task is to classify the area in the image as "Safe" or "Unsafe" based on visible indicators of security, safety, and livability from the perspective of someone of your gender.

Avoid assuming safety unless there is clear, strong, and visible evidence supporting a "Safe" classification. If prominent risks are observed, prioritize these concerns in your assessment and lean towards an "Unsafe" classification. Consider how someone of your gender would perceive the area. Also, consider the cumulative impact of multiple negative indicators on the overall perception of safety.

Provide your classification along with 3 specific keywords and a reason that accurately reflects the observed evidence justifying your choice. Organize your response in a JSON object with the following keys:

```
{
  "Classification": (your answer)
  "Keywords": (the 3 keywords)
  "Reason": (sentence that explains your choices)
}
```

Table S5. The Gender Prompt, instructing the model to assume a male or female perspective when evaluating urban safety.

Age Prompt

Assume the role of a young/middle-aged/elderly person. Your task is to classify the area in the image as "Safe" or "Unsafe" based on visible indicators of security, safety, and livability from the perspective of someone of your age.

Avoid assuming safety unless there is clear, strong, and visible evidence supporting a "Safe" classification. If prominent risks are observed, prioritize these concerns in your assessment and lean towards an "Unsafe" classification. Consider how someone of your age would perceive the area. Also, consider the cumulative impact of multiple negative indicators on the overall perception of safety.

Provide your classification along with 3 specific keywords and a reason that accurately reflects the observed evidence justifying your choice. Organize your response in a JSON object with the following keys:

```
{
  "Classification": (your answer)
  "Keywords": (the 3 keywords)
  "Reason": (sentence that explains your choices)
}
```

Table S6. The Age Prompt, instructing the model to adopt a young, middle-aged, or elderly perspective when evaluating urban safety.

S5. DISPARITIES IN MODEL OUTPUTS BASED ON THE SAME PROMPT TYPE

In this section, we present a selection of model-generated outputs to highlight how safety perception varies based on different socio-demographic personas. The results are summarized in Tables S7, S8, and S9, where we compare the classifications and justifications provided by the model when prompted with different nationalities, genders, and age groups.

By analyzing the model’s reasoning, we observe that safety perception is not uniform but instead reflects the attributes and biases associated with each socio-demographic profile. The explanations generated by the model reveal distinct patterns, highlighting how the safety perception is shaped by what the model considers characteristics of that particular socio-demographic group.

A. Nationality

Table S7. This table shows some random examples of disparities in the model classifications, keywords, and reasons for the same images using the nationality prompt.

Image ID	Nationality	Classification	Keywords	Reasons
50e5f7d4d7c3df413b00056d	Hong Kong	Unsafe	Gated, Fenced, Surveillance	The image shows a gated and fenced area, which may indicate restricted access or a need for security. The presence of surveillance cameras suggests that the area is monitored, possibly due to concerns about safety or crime. Additionally, the barren appearance of the street and the lack of visible people or activity could contribute to an overall perception of insecurity or disuse.
50e5f7d4d7c3df413b00056d	Singapore	Safe	Modern, maintained, Orderly	The image depicts a modern, well-maintained area with an orderly appearance. The presence of a large, clean building suggests that the area is likely to be well-managed and maintained. There are no visible signs of crime or disorder, which would indicate an unsafe environment. Additionally, the absence of any immediate threats or hazards further supports the classification of this area as safe.
50e5f7d4d7c3df413b00056d	South Africa	Unsafe	Deserted, Isolation	The image depicts a deserted, run-down building in an isolated area. The lack of people and the state of disrepair suggest that this location may not be considered safe for someone from South Africa’s perspective. The absence of visible security measures, such as fences or gates, further supports the classification of ‘Unsafe’. The overall impression is one of neglect and potential danger.

Image ID	Nationality	Classification	Keywords	Reasons
50f42b53fdc9f065f0001385	Romania	Unsafe	Deserted, Dilapidated, Neglected	The image depicts a deserted street with dilapidated buildings, which suggests neglect and lack of maintenance. This could indicate potential safety concerns such as criminal activity or an overall decline in the area's livability. The absence of people and vehicles on the street further supports this assessment.
50f42b53fdc9f065f0001385	Ukraine	Safe	Residential Area, Well-maintained, Low Crime	The image shows a residential area with well-maintained streets and buildings. There are no visible signs of crime or disorder, such as graffiti, broken windows, or littering. The presence of a clear roadway and the absence of any suspicious activity suggest that this neighborhood is likely safe for residents and visitors alike.
50f3981ffdc9f065f0000e0c	Italy	Safe	Quiet, Rural, Peaceful	The image depicts a quiet, rural area with no visible signs of danger or criminal activity. The presence of a few people and vehicles suggests that the area is inhabited and functional, but there are no indicators of conflict or immediate threat. The overall atmosphere appears peaceful and undisturbed, which would be appealing to someone from Italy seeking a calm environment.
50f3981ffdc9f065f0000e0c	Botswana	Safe	Rural, Deserted, Peaceful	The image depicts a rural area with no visible signs of danger or conflict. The absence of people and vehicles, along with the calmness of the scene, suggests that this location is peaceful and likely safe for residents and visitors alike. The lack of any indicators of crime or unrest further supports this classification.
50f3981ffdc9f065f0000e0c	Mexico	Unsafe	Deserted, Isolated, Rural	The image shows a deserted street with no visible people or activity. The lack of human presence and the absence of any discernible landmarks or urban features suggest that this area may be unsafe due to its isolation and potential for crime in rural settings. The desolate environment could also indicate a lack of basic services, such as law enforcement or emergency response, which would further contribute to an unsafe perception.

Figure S2 shows the hierarchical clustering of nationalities based on unsafe metrics (i.e., the average unsafe classified images and the standard deviation across cities). In this dendrogram, a red dashed line indicates the threshold used to cut the dendrogram and assign clusters.

Figure S3 displays the scatter plot where each point represents a nationality, color-coded by its cluster assignment. This plot further supports the clustering observed in the dendrogram.

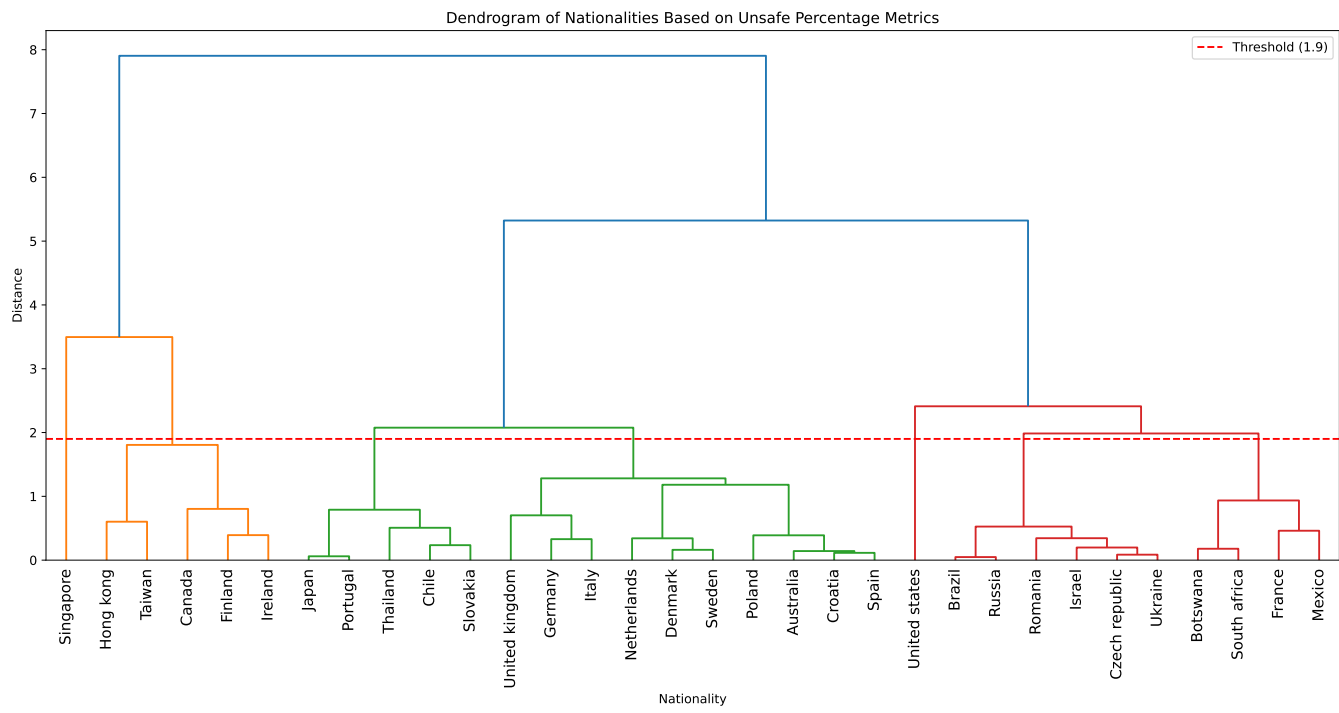


Figure S2. Hierarchical clustering of nationalities based on unsafe metrics (Average Unsafe Classified Images and Standard Deviation across cities). The red dashed line indicates the selected threshold for cluster division.

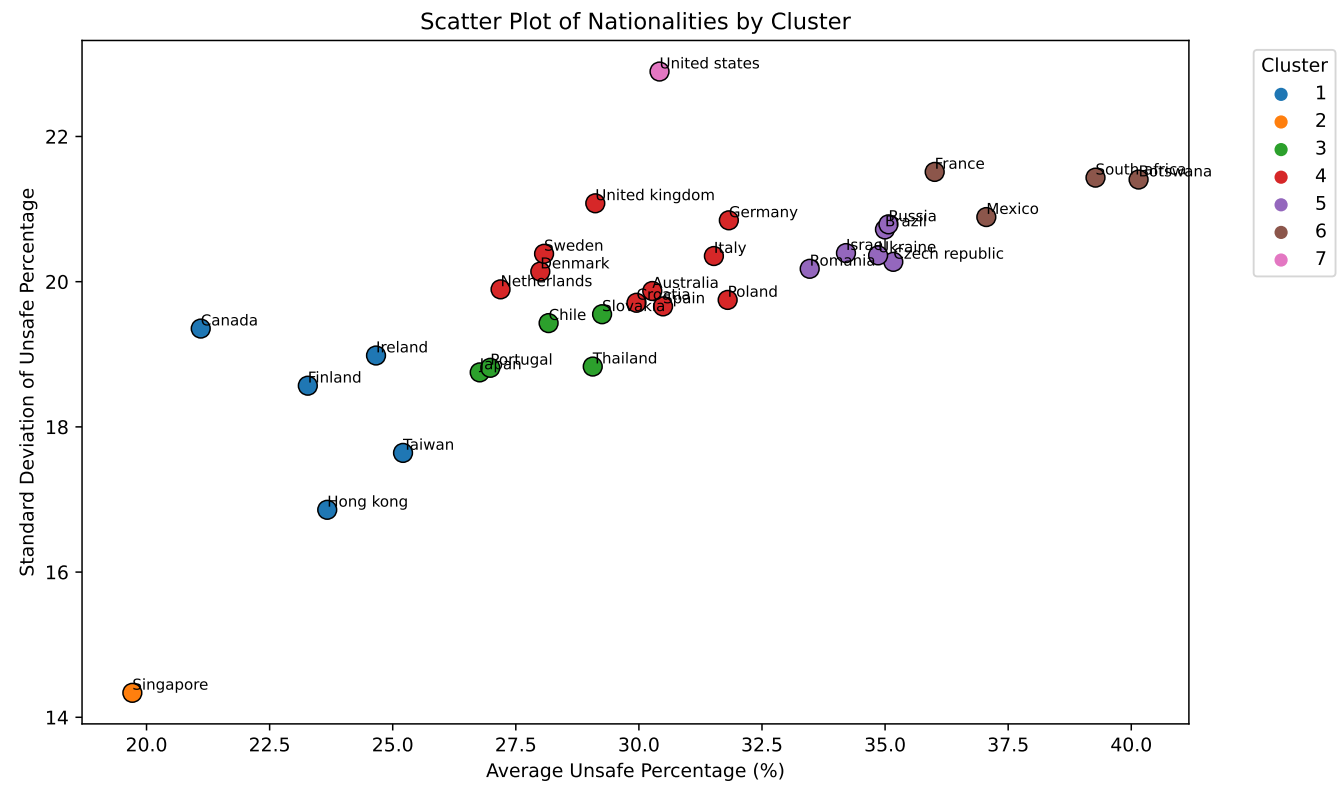


Figure S3. Scatter plot of nationalities by cluster. Each color corresponds to a different cluster as determined by the hierarchical clustering analysis.

B. Gender

Table S8. This table shows some random examples of disparities in the model classifications, keywords, and reasons for the same images using the gender prompt.

Image ID	Nationality	Classification	Keywords	Reasons
513d7b58fdc9f03587006b2c	Male	Safe	Residential, Neighborhood, Peaceful	The image depicts a quiet, residential neighbourhood with no visible signs of danger or criminal activity. The presence of houses and a tree-lined street suggests a peaceful environment where one might feel safe. There are no people in sight, which could be interpreted as either a lack of activity or a sense of privacy and security. However, the absence of any overtly negative indicators such as graffiti, broken windows, or abandoned buildings leans towards a classification of 'Safe'.
513d7b58fdc9f03587006b2c	Female	Unsafe	Modern, maintained, Orderly	The image depicts a modern, well-maintained area with an orderly appearance. The presence of a large, clean building suggests that the area is likely to be well-managed and maintained. There are no visible signs of crime or disorder, which would indicate an unsafe environment. Additionally, the absence of any immediate threats or hazards further supports the classification of this area as safe.
51413494fdc9f049260046e6	Male	Safe	Residential, Rural, Low Crime	The image depicts a rural residential area with a single-family home and a driveway. There are no visible signs of criminal activity or disorder, such as graffiti, broken windows, or abandoned vehicles. The presence of a well-maintained house suggests that the neighborhood is cared for by its residents. Additionally, the absence of any suspicious individuals or activities in the image indicates a low crime rate. Overall, the area appears to be safe and secure for someone of your gender.

Image ID	Nationality	Classification	Keywords	Reasons
51413494fdc9f049260046e6	Female	Unsafe	Isolated, Dilapidated, Deserted	The image depicts a desolate and abandoned area with no visible signs of security or maintenance. The presence of a dilapidated house, the absence of people, and the overall sense of neglect suggest that this location may not be considered safe for someone of your gender. The lack of clear indicators of safety, such as well-maintained infrastructure, active community engagement, or visible law enforcement presence, further supports the classification of 'Unsafe'.
514137c5fdc9f04926005041	Male	Safe	Residential, Neighborhood, Parked Cars	The image depicts a residential neighborhood with parked cars on both sides of the street. The presence of multiple vehicles suggests that this area is inhabited and possibly safe for residents and visitors alike. Additionally, there are no visible signs of danger or criminal activity, which further supports the classification as 'Safe'. However, it's important to note that a single image may not capture all aspects of safety in an area, and additional information would be needed to make a more comprehensive assessment.
514137c5fdc9f04926005041	Female	Unsafe	Vacant, Deserted, Lack of Maintenance	The image shows a deserted street with no visible people, cars parked haphazardly, and buildings that appear to be in disrepair. The lack of maintenance and the absence of people suggest a potential lack of safety and security in this area. These factors, when considered together, indicate an unsafe environment for someone of your gender.

C. Age

Table S9. This table shows some random examples of disparities in the model classifications, keywords, and reasons for the same images using the age prompt.

Image ID	Nationality	Classification	Keywords	Reasons
513e5fb9fdc9f0358700b2ad	Young	Safe	Urban, Residential, Well-maintained	The image depicts a well-maintained urban residential area with no visible signs of danger or neglect. The presence of parked cars and the orderly arrangement of buildings suggest that this is a safe neighborhood where residents feel secure enough to leave their vehicles unattended on the street. Additionally, there are no indicators of vandalism or disorder, which further supports the classification as 'Safe'. However, it's important to note that personal perception and experiences can greatly influence one's assessment of safety in a given area.
513e5fb9fdc9f0358700b2ad	Middle-Aged	Safe	Well-maintained, orderly, Secure	The image depicts a well-maintained urban area with orderly parking and no visible signs of vandalism or disorder. The presence of parked cars suggests that the neighborhood is safe enough for residents to leave their vehicles unattended. Additionally, there are no indicators of criminal activity or neglect, which would typically be associated with an unsafe environment.
513e5fb9fdc9f0358700b2ad	Elderly	Unsafe	Vehicle congestion, Parking issues, Abandoned buildings	From the perspective of an elderly person, the area in the image appears unsafe due to several factors. The presence of multiple vehicles parked haphazardly along the street suggests a lack of order and potential for accidents or theft. Additionally, the abandoned building indicates neglect and possible criminal activity. These factors combined create an environment that may be intimidating or dangerous for someone of elderly age.

Image ID	Nationality	Classification	Keywords	Reasons
51413d63fdc9f04926005d18	Young	Safe	Residential, Trees, Clear Sky	The image shows a residential area with trees lining the street, which can provide shade and a sense of community. The clear sky suggests good weather conditions, which are generally associated with safety and comfort. However, it is important to note that this assessment is based on a single image and does not account for other factors such as crime rates or general maintenance of the area.
51413d63fdc9f04926005d18	Middle-Aged	Unsafe	Deserted, Run-down, Isolation	The image depicts a deserted street with run-down houses, which suggests a lack of maintenance and potential neglect. The isolation indicated by the absence of people or activity in the area could also be perceived as unsafe for someone of middle age due to the increased risk of crime or emergency situations in such environments.
51413d63fdc9f04926005d18	Elderly	Unsafe	Empty streets, Lack of maintenance	The image shows an empty street with no visible people or activity, which could indicate a lack of community engagement or safety concerns. Additionally, the presence of bare trees and the overall appearance of neglect suggest that the area may not be well-maintained, which can contribute to feelings of insecurity for someone of elderly age.

S6. DATASET STATISTICS

Table S10. This table presents the number of images collected in each city, along with descriptive statistics of the *trueskill.score* (mean, standard deviation, minimum, and maximum)

City	Number images	Mean	Std	Min	Max
Amsterdam	23569	25.339	5.296	10.643	40.094
Atlanta	149258	25.259	5.202	10.283	41.149
Bangkok	58829	24.570	5.309	9.666	39.072
Barcelona	53317	25.111	5.114	11.746	39.624
BeloHorizonte	72704	24.296	5.279	9.290	38.842
Berlin	147407	25.170	5.098	10.954	39.639
Boston	49099	24.928	5.270	9.736	38.443
Bratislava	23643	25.218	5.077	11.738	39.321
Bucharest	80105	24.791	5.197	10.864	40.221
CapeTown	92980	25.309	5.102	9.858	38.191
Chicago	119029	25.217	5.291	10.154	40.343
Copenhagen	18537	24.932	5.073	12.604	37.684
Denver	88800	25.403	5.064	10.568	40.005
Dublin	58201	25.346	5.173	11.685	39.725
Gaborone	25493	24.986	5.482	10.864	38.581
Glasgow	35186	25.269	5.196	11.450	38.284
Guadalajara	57276	24.731	5.194	11.289	38.186
Helsinki	25419	25.030	5.143	12.346	39.979
HongKong	22903	24.667	5.267	11.749	37.646
Houston	114071	25.379	5.163	10.717	39.183
Johannesburg	69079	25.236	5.065	11.116	39.079
Kiev	32856	24.754	5.090	10.110	40.723
Kyoto	26677	25.053	5.317	12.278	39.815
Lisbon	69227	25.025	5.127	10.870	38.719
London	99234	25.201	5.341	10.175	40.298
LosAngeles	47878	24.829	5.024	10.774	39.545
Madrid	79772	25.166	5.049	10.629	39.393
Melbourne	100751	25.124	5.079	10.273	40.458
MexicoCity	77551	24.222	5.076	10.542	38.087
Milan	63636	24.999	5.140	9.452	41.164
Minneapolis	31154	25.534	4.880	11.921	38.992

City	Number images	Mean	Std	Min	Max
Montreal	96940	25.184	5.162	10.218	40.022
Moscow	106560	25.139	5.016	10.510	40.621
Munich	82362	25.457	5.031	8.867	39.464
NewYork	125726	24.687	5.225	10.325	40.658
Paris	91686	24.806	5.219	8.853	40.124
Philadelphia	102930	24.708	5.145	11.774	38.821
Portland	71372	25.186	5.090	11.770	43.441
Prague	64010	25.344	5.145	8.073	38.379
RioDeJaneiro	135381	24.175	5.322	9.680	39.843
Rome	80549	24.951	5.090	10.375	41.517
SanFrancisco	37666	24.650	5.038	13.167	38.008
Santiago	129426	24.597	5.163	9.603	39.332
SaoPaulo	110037	24.163	5.190	9.036	38.545
Seattle	55796	25.040	5.140	11.501	40.415
Singapore	96199	25.272	5.084	10.704	39.160
Stockholm	43438	25.010	5.081	12.110	38.805
Sydney	124282	25.008	5.006	11.011	40.709
Taipei	51282	24.601	5.303	10.732	38.571
TelAviv	23680	24.415	4.920	10.838	37.101
Tokyo	140082	24.893	5.157	11.157	38.930
Toronto	121619	25.435	5.140	10.859	39.772
Valparaiso	15836	24.202	5.150	11.712	36.445
Warsaw	110815	25.189	5.063	10.342	44.510
WashingtonDC	35224	25.410	5.404	12.067	39.666
Zagreb	39997	25.160	5.073	9.452	38.160

Table S11. City-Nation Mapping in Place Pulse 2.0

City	Nation
Amsterdam	Netherlands
Atlanta	United States
Bangkok	Thailand
Barcelona	Spain
Belo Horizonte	Brazil
Berlin	Germany
Bratislava	Slovakia
Boston	United States
Bucharest	Romania
Cape Town	South Africa
Chicago	United States
Copenhagen	Denmark
Denver	United States
Dublin	Ireland
Glasgow	United Kingdom
Gaborone	Botswana
Guadalajara	Mexico
Hong Kong	Hong Kong
Houston	United States
Johannesburg	South Africa
Kyoto	Japan
Kyiv	Ukraine
Lisbon	Portugal
London	United Kingdom
Los Angeles	United States
Madrid	Spain
Melbourne	Australia
Milan	Italy
Minneapolis	United States

City	Nation
Montreal	Canada
Moscow	Russia
New York	United States
Philadelphia	United States
Portland	United States
Prague	Czech Republic
Rio de Janeiro	Brazil
Rome	Italy
San Francisco	United States
Sao Paulo	Brazil
Santiago	Chile
Seattle	United States
Singapore	Singapore
Stockholm	Sweden
Tel Aviv	Israel
Taipei	Taiwan
Tokyo	Japan
Toronto	Canada
Valparaiso	Chile
Washington DC	United States
Warsaw	Poland
Zagreb	Croatia